Recognition of Regular-shaped Objects by Single Camera Views Using Camera Calibration, Surface Backprojection, and Model Matching Techniques

Cheng-Hsiung Liu（劉政雄） and Wen-Hsiang Tsai （蔡文祥）@

Institute of Computer Science and Information Engineering
Department of Computer and Information Science
National Chiao Tung University
Hsinchu, Taiwan 300
Republic of China

Abstract

A new approach to recognition of regular-shaped objects by single camera views using both object shape and surface pattern information is proposed. The recognized objects are regular prisms of different sizes. Both the silhouette shape and the surface pattern of the object are utilized in the recognition scheme. To recognize an input object, a new camera calibration technique is first employed to compute the camera parameters and the object dimension parameters analytically using a single camera view of the object. A surface backprojection technique is then adopted to reconstruct the pattern on each surface patch of the input object. Finally, each surface patch pattern is matched with those of each object model using the distance weighted correlation measure. Experimental results showing the feasibility of the proposed approach are also included.

Key Words : object recognition, regular prisms, camera calibration, surface backprojection, model matching, surface patterns, distance weighted-correlation.

I. Introduction

In this section, a survey of related works is first given, followed by a description of an overview of the proposed approach.

1.1 Survey

In industrial automation tasks, such as bin picking, sorting of machine parts, automatic assembling, and automatic warehousing, it is often found necessary to recognize 3D objects. Most related research works focus on recognizing 3D objects using silhouette shape information only; object surface patterns such as special marks or characters are less utilized. In this study, both object silhouette shapes and surface patterns are used to recognize 3D objects more effectively.

Chin and Dyer[1] presented a good survey of model-based computer vision works, and Besl and Jain[2] reviewed a lot of 3D object recognition systems. In recent years, many more 3D recognition systems were proposed. According to the matching methods used, 3D object recognition can be classified into two types: 3D recognition by 3D matching, and 3D recognition by 2D matching.

In the approaches[3-6] of the first type, it is usually necessary to acquire 3D object surface data from the input intensity image[3-4, 6] or range image[5], and before the final recognition step can be performed, they must be transformed into certain 3D representations. In the approaches of this type, 3D data acquisition and object modeling works usually take long computation time which causes such approaches inapplicable to many applications.

The other contrastive type[7-9] of approaches is 3D recognition by 2D matching. Some of them are reviewed briefly here. Silberberg et al.[7] used the general Hough transform technique to match input 2D line segments and edge junctions with 3D model line segments and vertices. For each pair of line segments being matched, the model line is projected onto the image line, incrementing the corresponding cell in the Hough accumulator array if the matching is successful. Liu and Tsai[8] proposed a 3D curved object recognition system including a turn-table, a top-view camera, and a lateral-view camera. A 3D object was recognized by first normalizing the orientation and position of the top-view silhouette shape by its principal axis and centroid, and then matching the shape features of the 2D silhouette shapes of the input object against those of each object model by traversing a decision tree.

A common property of the previously-mentioned approach is that input 3D objects are

@ To whom all correspondence should be sent.

recognized by matching the processed input object images or representations against 2D reference object models. This is why such approaches are said to be of the type of 3D recognition by 2D matching. An advantage of this type of approach is that well-developed 2D image or shape analysis techniques can be utilized. However, extra effort must be paid to avoid exhaustive matching of the input 2D data with the essentially infinite number of possible 2D views of each 3D reference object. In this paper, we propose a new approach to 3D object recognition which is basically a combination of the above two types of approaches but without their disadvantages.

1.2 Overview of Proposed Approach

In this study, it is desired to utilize not only the object silhouette shape but also the object surface pattern to recognize 3D regular-shaped objects. The reason is that a lot of commercial products, especially those packed with paper boxes, are regular-shaped, and have abundant gray-scale or color pattern information on their surface patches which can be utilized in recognition. The regular-shaped object investigated in this study is the regular prism. A prism is a polyhedron with two congruent and parallel base faces, and several lateral faces which are parallelograms formed by joining corresponding vertices of the bases. A regular prism is a prism with its top and bottom bases being identical regular polygons and perpendicular to the lateral faces. A regular polygon is a polygon that all of its sides and all of its interior angles are equal. Some examples of regular prisms are shown in Fig. 1. In this sequel, let n denote the number of the boundary line segments of the regular polygon of the top or bottom base of the regular prism, where $n > 3$. On the other hand, it is also desired to recognize objects in arbitrary orientations by single views, just like what human beings do in observing and recognizing objects. This will increase the applicability of the recognition scheme. The first step to accomplish these goals is to reconstruct the 2D object surface patterns, which are deformed in the input image due to perspective transformation in the imaging process. For this purpose, a new camera calibration technique is proposed, which can be performed in an on-line fashion, followed by the use of a surface backprojection technique. After the 2D surface patterns are obtained, object recognition are proceeded using a well-developed 2D pattern matching method.

More specifically, an object to be recognized is put on a flat surface within the field of view of a TV camera at a known fixed height. The orientation and position of the object with respect to the camera can be arbitrary. Image processing techniques are then applied to extract the boundary and edge lines of the object surface in the image. These lines come from the intersections of the flat surface patches of the object. Seven of these edge lines are used to compute the camera parameters. The principle behind the proposed camera calibration process is that the angles formed by these lines as well as the lengths of these lines (actually, of these line segments) contain abundant information about the position and the orientation angles of the camera (i. e., about the camera parameters). Analytical solutions for the camera parameters have been derived in this study for fast computation which speeds up on-line object recognition.

After the camera parameters are computed, a surface backprojection technique is employed to compute the 3D coordinates of the pattern points on each surface patch of the input object. From these 3D data, 2D surface patterns are then reconstructed. Finally, the 2D patterns of all the input object surface patches are matched against those of each object model, which are constructed in the learning phase, to classify the input object according to a computed similarity measure.

Advantages of the proposed approach include at least the following.

(1) Only a single view of each object is required for recognizing an object. This reduces the recognition time of each object.

(2) An object to be recognized can be placed in an arbitrary orientation; no special view angle with respect to the camera need be assumed for the object. This enhances the flexibility of the system setup and the applicability of the proposed approach.

(3) The formulas derived for computing the camera parameters are analytic, making parameter computation works faster and on-line 3D data acquisition possible. This contrasts with most approaches of the type of 3D recognition by 3D matching, which usually spend large amounts of time in 3D data acquisition and transformation.

(4) Since not only object silhouette shapes but also object surface patterns are utilized in the recognition scheme, more object features can be extracted and higher recognition rates can be achieved.

(5) Well-developed 2D shape matching can be applied easily because the model matching step is essentially a simple process of 2D pattern comparison.

(6) Both the learning and recognition phases follow an identical procedure. This reduces the complexity of the proposed approach.

In the remainder of the paper, the camera calibration and surface backprojection techniques are first described. Detailed discussions on the object learning and recognition procedures follow next. Experimental results and conclusions are presented finally.

II Proposed Camera Calibration Technique

For the convenience of explanation, the regular prism with its top or bottom surface being a regular hexagon (i. e., $n = 6$) is employed as the example. For other types of regular prisms (with n

≠ 6) similar results can be derived using similar procedures. The details are omitted.

Fig. 2 shows the global coordinate system associated with a regular prism with regular hexagon bases. Let lines L_1, L_2, and L_3 be the X-, Y-, and Z-axes, respectively. The origin of the global coordinate system is the intersection point of the X-, Y-, and Z-axes.

The camera location with respect to the global coordinate system is represented by three position parameters X_c, Y_c, and Z_c and three orientation parameters φ, θ, and δ, where φ, θ, and δ are called the Eulerian angles or the pan, tilt, and swing angles of the camera, respectively. In this study, it is assumed that the parameter Z_c is known in advance, and it is desired to solve the remaining five camera parameters as well as two dimension parameters of the regular prism (the height b of the prism and the side length a of the top or bottom base as shown in Fig. 2) in terms of the equation coefficients of seven boundary lines of the surface patches of the regular prism as well as those of the corresponding image lines. The lines L_1 through L_7 (including two virtual lines L_2 and L_7) used here are shown in Fig. 2. Note that L_2 is just the Y-axis.

The proposed method for camera calibration consists mainly four steps: (1) derivations of the line equations of L_1', and L_3' through L_7' from the image; (2) derivation of the line equation of L_2' using those of L_1', L_6', and L_7'; (3) derivations of the camera orientation parameters φ, θ, and δ using the line equations of L_1', L_2', and L_3'; (4) derivations of the other camera parameters X_c, Y_c, and the dimension parameters (a and b) of the regular prism using the line equations of L_1' through L_7'. The following are the details of the steps (the details are omitted).

Step 1. Derivations of the line equations of L_1', and L_3' through L_7' from the image

Referring to Fig. 5.3(b), by using image processing techniques, the coordinates of the corner points $A'(A_x', A_y')$, $B'(B_x', B_y')$, $C'(C_x', C_y')$, $D'(D_x', D_y')$, $E'(E_x', E_y')$, and $O'(O_x', O_y')$ in the image plane can be found.

Let the line equation of L_i' be

$$U + b_i' V + c_i' = 0, \qquad i=1, 2, 3, 4, 5, 6, 7 \quad (1)$$

the b_i' and c_i' (i=1, 3, 4, 5, 6, 7) can be found using simple geometry from the coordinates of the corner points in Fig. 5(b).

Step 2. Derivation of the line equation of L_2' using those of L_1', L_6', and L_7'

From the coefficients of the line equations of L_1', L_6', and L_7', the coefficients of the line equation of L_2' which is the projection of the Y-axis (L_2) can be obtained. After the line equation of L_2' are solved, the camera orientation parameters φ, θ, and δ can be derived using the line equations of L_1', L_2', and L_3'.

Step 3. Derivations of the camera orientation parameters φ, θ, and δ using the line equations of L_1', L_2', and L_3'

The parameters φ, θ, and δ can be derived as follows (the details are omitted):

$$\tan\delta = \frac{-B_1 - \sqrt{B_1^2 - 4A_1C_1}}{2A_1}, \quad (2)$$

$$\tan\theta = \frac{c_3}{f(b_3\cos\delta - \sin\delta)}, \quad (3)$$

$$\tan\varphi = \frac{fb_1\sin\delta + f\cos\delta}{fb_1\cos\theta\cos\delta - f\cos\theta\sin\delta + c_1\sin\theta}, \quad (4)$$

where

$$A_1 = f^2c_3^2b_1b_2 + c_3^2c_1c_2 + f^2c_1c_2 + f^2c_2c_3 + f^4(1 + b_1b_2),$$

$$B_1 = f^2c_3^2(b_1 + b_2) - f^2c_3c_1(b_2 + b_3) - f^2c_3c_2(b_3 + b_1) - 2f^4b_3(1 + b_1b_2),$$

$$C_1 = f^2c_3^2 + c_3^2c_1c_2 + f^2c_3c_1b_2b_3 + f^2c_3c_2b_3 + f^4(1 + b_1b_2) + f^4(1 + b_1b_2)b_3^2.$$

So from the information of the line equations of the projection lines L_1', L_2', and L_3' of the X-, Y- and Z-axes, respectively, the camera orientation parameters φ, θ, and δ can be derived.

Step 4. Derivations of other camera parameters X_c, Y_c, and the dimension parameters of the regular prism from the line equations of L_1' through L_7'

As shown in Fig. 2, the side length of the top hexagon base and the height of the regular prism are a and b, respectively.

Since only one image is taken, the scaling factor problem cannot be solved unless one of the six camera parameters is known. For this, recall the assumption we made before that the camera height Z_c, which is the distance between the origin point O of the global coordinate system and the origin point C of the camera coordinate system, is given.

With Z_c given, the other five camera parameters and the values of a and b can all be solved using the equations of the seven lines L_1 through L_7 shown in Fig. 2 as follows (the details are omitted).

$$X_c = \frac{\Delta_6}{\Delta_5} Y_c = \frac{\Delta_2 \Delta_6}{\Delta_1 \Delta_5} Z_c, \tag{5}$$

$$Y_c = \frac{\Delta_2}{\Delta_1} Z_c, \tag{6}$$

$$a = (1 - \frac{\Delta_5 \Delta_8}{\Delta_6 \Delta_7}) \frac{\Delta_2 \Delta_6}{\Delta_1 \Delta_5} Z_c, \tag{7}$$

$$b = (\frac{\Delta_1 \Delta_4 - \Delta_2 \Delta_3}{\Delta_1 \Delta_4}) Z_c = (1 - \frac{\Delta_2 \Delta_3}{\Delta_1 \Delta_4}) Z_c, \tag{8}$$

where

$$\begin{aligned}
\Delta_1 &= \sin\theta\cos\delta + b_1 \sin\theta\sin\delta, \\
\Delta_2 &= \sin\varphi\sin\delta + \cos\varphi\cos\theta\cos\delta \\
&\quad + b_1 \sin\varphi\cos\theta\sin\delta - b_1 \sin\varphi\cos\delta, \\
\Delta_3 &= \sin\theta\cos\delta + b_4 \sin\theta\sin\delta, \\
\Delta_4 &= \sin\varphi\sin\delta + \cos\varphi\cos\theta\cos\delta \\
&\quad + b_4 \sin\varphi\cos\theta\sin\delta - b_4 \sin\varphi\cos\delta, \\
\Delta_5 &= b_3 \sin\varphi\cos\delta - b_3 \cos\theta\sin\delta - \sin\varphi\sin\delta \\
&\quad - \cos\varphi\cos\theta\cos\delta, \\
\Delta_6 &= \sin\varphi\cos\theta\cos\delta + b_3 \cos\varphi\cos\delta \\
&\quad + b_3 \sin\varphi\cos\theta\sin\delta - \cos\varphi\sin\delta, \\
\Delta_7 &= b_5 \sin\varphi\cos\delta - b_5 \cos\theta\sin\delta \\
&\quad - \sin\varphi\sin\delta - \cos\varphi\cos\theta\cos\delta, \\
\Delta_8 &= \sin\varphi\cos\theta\cos\delta + b_5 \cos\varphi\cos\delta \\
&\quad + b_5 \sin\varphi\cos\theta\sin\delta - \cos\varphi\sin\delta.
\end{aligned}$$

Therefore, with Z_c given, X_c, Y_c, a, and b can all be solved using Eqs. (5), (6), (7), and (8), respectively. Note that for other n values (i.e., for regular prisms with top bases other than hexagons), the above derivation procedure is still applicable with minor modifications. Note also that the derivations of the values of a and b in the above procedure in addition to the camera parameters make it possible to recognize regular prisms of different sizes.

III Method For Reconstructing Surface Patch Patterns Using Backprojection Technique

Once the camera parameters have been solved, we can reconstruct the pixel data of the surface patch patterns using a surface backprojection technique. In Fig. 4, let the coordinates of any point P in the image plane be (a, b). Then its coordinates in the camera coordinate system are (a, b, f). The line L_1 passing through the origin C of the camera coordinate system and point P is called the backprojection line of P. By the principle of backprojection, the coordinates of any point P' on the backprojection line L_1 can be specified by (at, bt, ft) with t as a free variable. Let (x, y, z) be the desired corresponding coordinates in the global coordinate system. Then, we get

$$(at, bt, ft, 1) = (x, y, z, 1) \begin{bmatrix} V_1 & V_2 & V_3 & 0 \\ V_4 & V_5 & V_6 & 0 \\ V_7 & V_8 & V_9 & 0 \\ O_1 & O_2 & O_3 & 1 \end{bmatrix}, \tag{9}$$

from which we can derive the following three equations (the details are omitted):

$$x = X_1 t + X_2 = \frac{m_2}{m_1} t - \frac{m_5}{m_1}, \tag{10}$$

$$y = Y_1 t + Y_2 = \frac{m_3}{m_1} t - \frac{m_6}{m_1}, \tag{11}$$

$$z = Z_1 t + Z_2 = \frac{m_4}{m_1} t - \frac{m_7}{m_1}, \tag{12}$$

where

$$X_1 = \frac{\begin{bmatrix} a & V_4 & V_7 \\ b & V_5 & V_8 \\ f & V_6 & V_9 \end{bmatrix}}{\begin{bmatrix} V_1 & V_4 & V_7 \\ V_2 & V_5 & V_8 \\ V_3 & V_6 & V_9 \end{bmatrix}} = \frac{m_2}{m_1},$$

$$X_2 = \frac{-\begin{bmatrix} O_1 & V_4 & V_7 \\ O_2 & V_5 & V_8 \\ O_3 & V_6 & V_9 \end{bmatrix}}{\begin{bmatrix} V_1 & V_4 & V_7 \\ V_2 & V_5 & V_8 \\ V_3 & V_6 & V_9 \end{bmatrix}} = \frac{-m_5}{m_1},$$

$$Y_1 = \frac{\begin{bmatrix} V_1 & a & V_7 \\ V_2 & b & V_8 \\ V_3 & f & V_9 \end{bmatrix}}{\begin{bmatrix} V_1 & V_4 & V_7 \\ V_2 & V_5 & V_8 \\ V_3 & V_6 & V_9 \end{bmatrix}} = \frac{m_3}{m_1},$$

$$Y_2 = \frac{-\begin{bmatrix} V_1 & O_1 & V_7 \\ V_2 & O_2 & V_8 \\ V_3 & O_3 & V_9 \end{bmatrix}}{\begin{bmatrix} V_1 & V_4 & V_7 \\ V_2 & V_5 & V_8 \\ V_3 & V_6 & V_9 \end{bmatrix}} = \frac{-m_6}{m_1}..$$

$$Z_1 = \frac{\begin{bmatrix} V_1 & V_4 & a \\ V_2 & V_5 & b \\ V_3 & V_6 & f \end{bmatrix}}{\begin{bmatrix} V_1 & V_4 & V_7 \\ V_2 & V_5 & V_8 \\ V_3 & V_6 & V_9 \end{bmatrix}} = \frac{m_4}{m_1} ,$$

$$Z_2 = \frac{-\begin{bmatrix} V_1 & V_4 & O_1 \\ V_2 & V_5 & O_2 \\ V_3 & V_6 & O_3 \end{bmatrix}}{\begin{bmatrix} V_1 & V_4 & V_7 \\ V_2 & V_5 & V_8 \\ V_3 & V_6 & V_9 \end{bmatrix}} = \frac{-m_7}{m_1} .$$

In the above equations, the free variable t remains unsolved. If the point lies on the surface of the regular prism, then t can be solved according to the following procedure.

As can be seen from Fig. 5, any point, which lies on the surface of the regular prism and can be seen in the image, must lie on one of the four surface patches, i. e., on patch 0, patch 1, patch 2, or patch 3. Assume first that point P' with the global coordinates (x, y, z) lies on patch 0. Then $y \geq 0$ and $z = b$. From the constraint $z = b$, the free parameter t can be solved using Eq. (12) (the details are omitted) to be

$$t = \frac{m_1 b + m_7}{m_4} , \qquad (13)$$

where m_1, m_4, and m_7 are given in Eq. (12).

After substituting the value of t into Eqs. (10), (11), and (12) to get the values of x, y, and z, we can check if $y \geq 0$ is satisfied. If so, then point P' is assured to lie on patch 0. If not, then point P' must lie on patch 1, patch 2, or patch 3. Once again, assume that point P' lies on patch 1, then it is easy to derive the constraints $y = -x*\tan(\pi/3)$, $-a\cos(\pi/3) \leq x \leq 0$, $0 \leq y \leq a\sin(\pi/3)$, and $0 \leq z \leq b$. From the constraint $y = -x*\tan(\pi/3)$, the free parameter t can be solved to be

$$t = \frac{m_6 + \tan(\pi/3)m_5}{m_3 + \tan(\pi/3)m_2} , \qquad (14)$$

where m_2, m_3, m_5, and m_6 are given in Eqs. (10) and (11).

By the same process, we can check if $-a\cos(\pi/3) \leq x \leq 0$, $0 \leq y \leq a\sin(\pi/3)$, and $0 \leq z \leq b$ are satisfied. If so, then point P' is assured to lie on patch 1, else it must lie on patch 2 or patch 3. Assume that point P' lies on patch 2, then $0 \leq x \leq a$, $y = 0$, $0 \leq z \leq b$. From the constraint $y = 0$, the free parameter t can be solved, using Eq. (11), to be

$$t = \frac{m_6}{m_3} , \qquad (15)$$

where m_3 and m_6 are given in Eq. (11).

By a similar process, we can check if $0 \leq x \leq a$ and $0 \leq z \leq b$ are satisfied. If so, then point P' is assured to lie on patch 2. If not, then point P' must lie on patch 3, and the constraints $y = x*\tan(\pi/3)$, $0 \leq x \leq a\cos(\pi/3)$, $0 \leq y \leq a\sin(\pi/3)$, and $0 \leq z \leq b$ must be satisfied. From the constraint $y = x*\tan(\pi/3)$, t can be solved to be

$$t = \frac{m_6 + \tan(\pi/3)m_5}{m_3 + \tan(\pi/3)m_2} ,$$

where m_2, m_3, m_5, and m_6 are given in Eqs. (10) and (11).

We can check further if $0 \leq x \leq a\cos(\pi/3)$, $0 \leq y \leq a\sin(\pi/3)$, and $0 \leq z \leq b$ are satisfied. If so, then point P' is assured to lie on patch 3.

From each of the above cases, the free variable t can be solved for each point P' lying on the surface of the regular prism after determining which surface patch P' lies on, and the 3D coordinates (x, y, z) of point P' in the global coordinate system can then be determined according to Eqs. (10) through (12). This completes the backprojection process for point P.

After the 3D coordinates of all points are determined, the points have also been grouped according to which surface patch they lie on, and we can reconstruct each group into a 2D point pattern according to the following procedure.

Referring to Fig. 6(a), let the 3D coordinates of points P_1, P_2, and P_3 on patch 1, patch 2, and patch 3 be (x_1, y_1, z_1), (x_2, y_2, z_2), and (x_3, y_3, z_3), respectively. It is desired to reconstruct the coordinates of P_i (i = 1, 2, 3) in the 2D M-N plane as shown in Fig. 6(b). Let the reconstructed 2D coordinates of points P_1, P_2, and P_3 on the M-N plane be $P'_1(m_1, n_1)$, $P'_2(m_2, n_2)$, and $P'_3(m_3, n_3)$, respectively. Then according to simple geometry, $m_1 = -\sqrt{x_1^2 + y_1^2}$, $n_1 = z_1$, $m_2 = x_2$, $n_2 = z_2$, $m_3 = a + \sqrt{(x_3 - a)^2 + y_3^2}$, and $n_3 = z_3$. This completes the process for reconstructing the surface patch patterns using the backprojection technique.

The binary values of each group of points form a 2D point pattern for a surface patch, which can then be used for object recognition as described in the next section.

IV Learning and Recognition Phases

4.1 Learning Phase

First, if there is any model to be built, an appropriate view of the model object is taken. Image processing operations (thresholding, edge detection, thinning, and line detection) are then applied to the image to get the line boundary and the point patterns of the surface patches of the regular prism. The coefficients of the equations of the seven lines (L_1 through L_7) are also found, and the camera parameters and the dimension parameters of the regular prism computed. The surface patch patterns of the regular prism then are reconstructed using the surface backprojection technique.

4.2 Recognition Phase

The recognition phase starts from the camera calibration procedure. That is, each time an object is to be recognized, the type of regular prism(i. e., the value of n) and the camera parameters are found out first. The value of n can be computed as follows. Let c denote the number of the corner points of the boundary of the regular prism obtained by corner detection, then n = c - 2. After the calibration step, each surface patch is reconstructed accordingly. Then in the step of matching, the computed top-polygonal side length and the height of the regular prism are used first to reject inappropriate surface patches in the object model. Then, a similarity value, based on the distance weighted correlation (DWC) function[10], between each of the surface patch patterns of the input object and each of those of each object model is computed to decide if the surface patch patterns match well. If all the surface patch patterns match with those of a certain object, say A, in the object model, then we conclude that the object being recognized is object A. Otherwise, we decide that the object is unknown. In this way, regular prisms of different sizes with different surface patch patterns can be recognized.

The similarity measure employed in this approach is the DWC function with search distance = $2\sqrt{2}$ and window size 5x5. This measure is appropriate for matching point patterns. The detailed information of the DWC function can be found in Fan and Tsai[22].

V Experimental Results

Some experiments have been conducted on an IBM PC with an 80286 processor using a CCD TV camera. Figure 7 shows the diagram of the experimental environment. Once the environment has been set up, the parameters Z_c and f are fixed. Regular prisms of different with different surface patterns to be recognized are placed on the table and are recognized using fixed values of Z_c and f. To compute the exact values of f and Z_c, a regular prism of known size (with dimension parameters a_1 and b_1) is used as a calibration object first. Then Z_c and f are estimated roughly. By using these rough values of Z_c and f and setting a reasonable search range (15%) around Z_c and f, Eqs (7) and (8) are used to compute the dimension parameters (denoted as a_2 and b_2) of the regular prism iteratively until the difference between a_1 and a_2 and that between b_1 and b_2 are both within some tolerance. The resulting values of Z_c and f are then taken as the exact values. Once the exact values of Z_c and f are then obtained, any regular prism can be recognized accordingly as long as the environment remains unchanged.

To show the feasibility of the approach, three regular prisms with hexagon bases were recognized. Since the proposed method can identify the type of regular prism(i. e., get the value of n) and also compute the dimension parameters of the regular prism, regular prisms of different types and different sizes can be discriminated immediately. Therefore, only regular prisms of identical sizes but with different surface patch patterns were used in the experiments. The surface patterns of the objects include English characters, numbers, and geometrical patterns. Figures 8(a) - (c) are the results of preprocessing the image of regular prism 1 with character patterns on its surface patches. Figure 8(d) is the result of reconstructing the surface patch patterns of regular prism 1. Due to possible errors in the preprocessing step, distortion occurs in the reconstructed surface patch patterns of the regular prism; the boundaries of some surface patches were not well reconstructed. But such errors usually do not influence the result of the following surface pattern matching process because the patch boundaries, which are not essential information for object discrimination, were removed in our experiments before surface pattern matching. Table 1 includes the results of the computed camera parameters and the dimension parameters of the regular prisms. From the table, we see that the errors of the computed regular prism dimension parameters are less than 5 %. Table 2 includes the results of the computed DWC measures between the surface patch patterns of the objects to be recognized and those of the object models. Each surface patch of each regular prism is assigned correctly. As the results show, the three regular prisms with different surface patch patterns were all recognized correctly.

VI Conclusions

A new approach to 3D regular-shaped object using both object shape and surface pattern information has been proposed. Experimental results have been shown to prove the feasibility of the approach. The approach consists of the steps of on-line camera calibration, backprojection for object surface reconstruction, and surface pattern matching for object recognition. Regular prisms in arbitrary orientations can be recognized using single camera views. This increases the flexibility of the proposed approach. The analytic solutions of the

camera parameters speed up the camera calibration process. The use of the computed object size and surface patch patterns improves the discrimination capability of the proposed approach.

References

[1] R. T. Chin and C. R. Dyer, "Model-based recognition in robot vision," *Computing Surveys*, Vol. 18, no. 1, pp. 67-108 ,1986.

[2] J. Besl and R. C. Jain, "Three-dimensional object recognition," *Computing Surveys*, Vol. 17, no. 1, pp. 75-145, 1985.

[3] M. Oshima and Y. Shirai, "Object recognition using three-dimensional information," *IEEE Trans. Pattern Analysis and Machine Intelligence*, Vol. PAMI-5, no. 4, pp. 353-361, 1983.

[4] R. A. Brooks, "Model-based three dimensional interpretations of two-dimensional images,' *IEEE Trans. Pattern Analysis and Machine Intelligence*, Vol. PAMI-5, no. 2, pp. 140-150, 1983.

[5] J. K. Aggarwal and M. J. Magee, "Determining Motion parameters using intensity guided range sensing," *Pattern Recognition*, Vol. 19, no. 2, pp. 169-180, 1986.

[6] D. P. Huttenlocher and S. Ullman, "Recognizing solid objects by alignment with an image," *International Journal of Computer Vision*, Vol. 5, no. 2, pp. 195-212, 1990.

[7] T. M. Silberberg, L. Davis, and D. Harwood, "An iterative Hough procedure for three-dimensional object recognition," *Pattern Recognition*, Vol. 17, no. 6, pp. 621-629, 1984.

[8] C. H. Liu and W. H. Tsai, "3D curved object recognition from multiple 2D camera views," *Computer Vision, Graphics, and Image Processing*, Vol. 50, pp. 177-187, 1990.

[9] M. C. Yang and W. H. Tsai, "Recognition of single 3D curved objects using 2D cross-sectional slice shapes," *Image and Vision Computing*, Vol. 7, no. 3, pp. 210-216, 1989.

[10] T. J. Fan and W. H. Tsai, "Automatic Chinese seal identification," *Computer Vision, Graphics and Image Processing* 25, pp. 311-330, 1984.

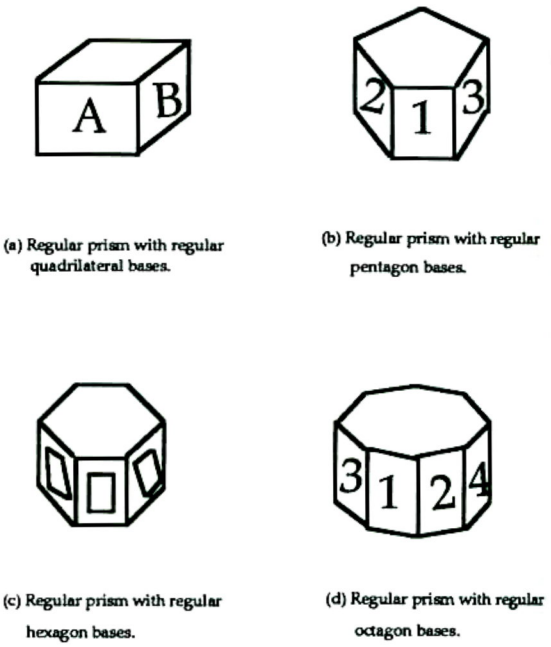

(a) Regular prism with regular quadrilateral bases.

(b) Regular prism with regular pentagon bases.

(c) Regular prism with regular hexagon bases.

(d) Regular prism with regular octagon bases.

Fig. 1 Some examples of regular prisms investigated in the proposed approach.

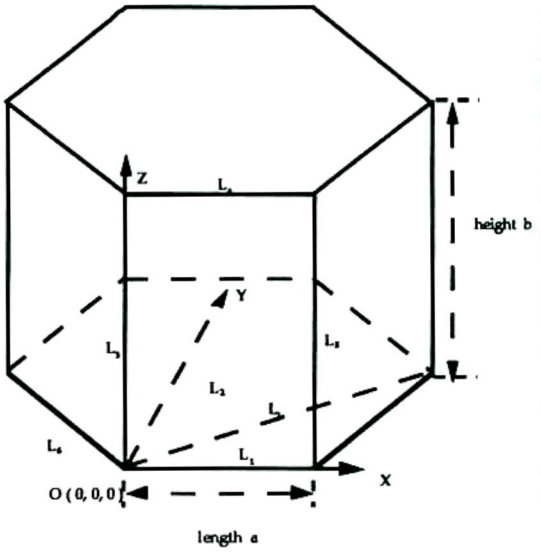

Fig. 2 The global coordinate system attached on a regular prism with hexagon bases to be recognized.

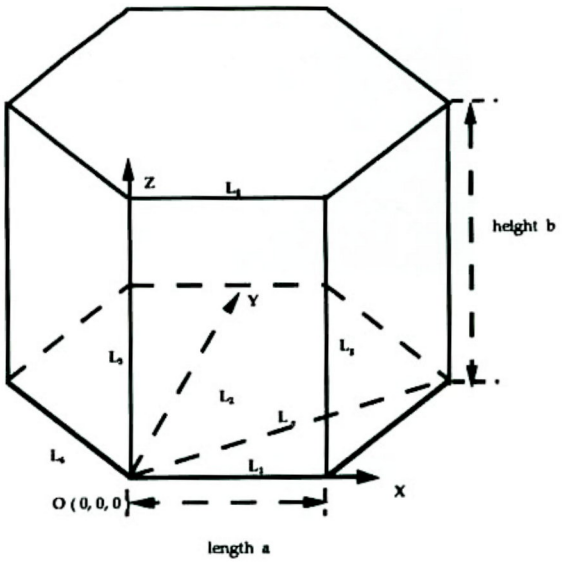

(a) The lines and their corresponding polar space angles.

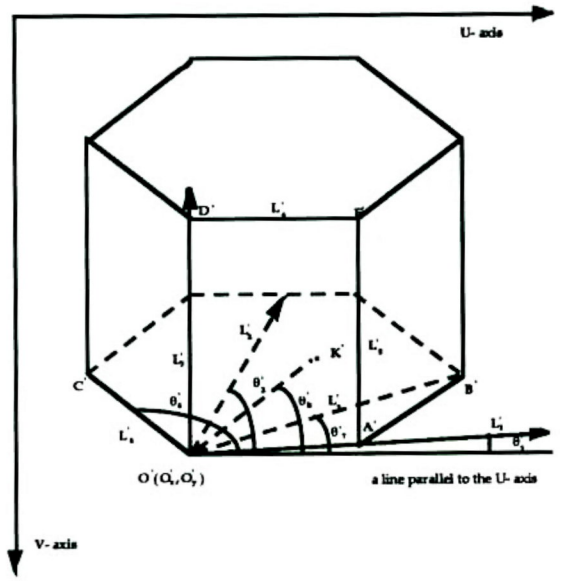

(b) The corresponding lines and the polar image angles of (a).

Fig. 3 A regular prism with hexagon bases and its image.

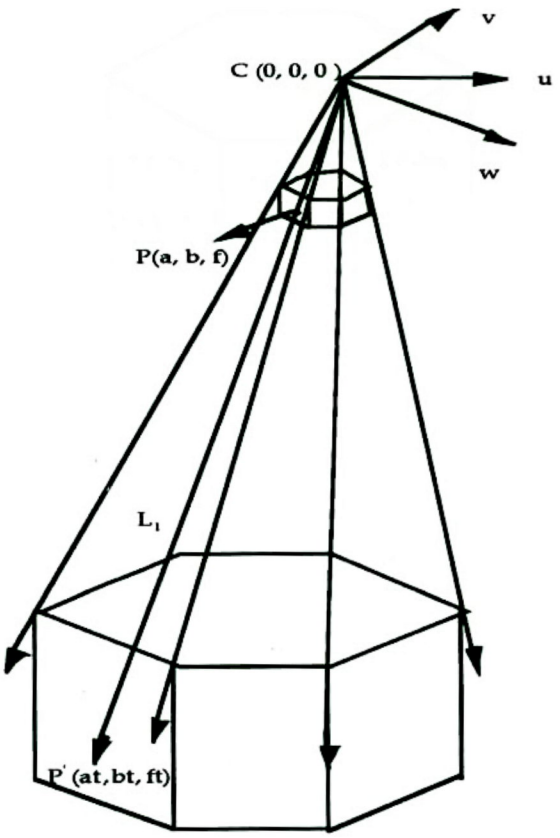

Fig. 4 Illustration of the backprojection procedure.

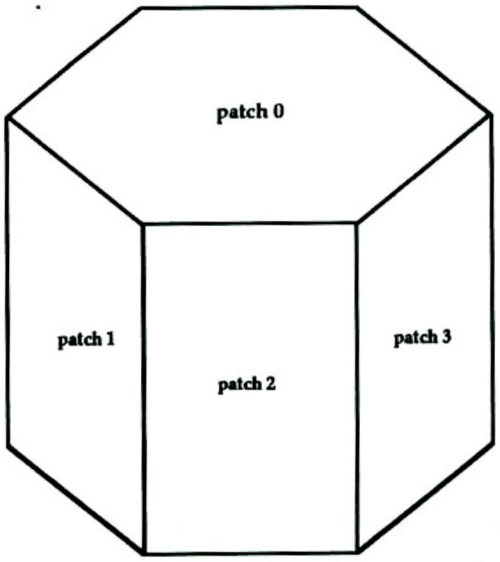

Fig. 5 The four surface patches on a regular prism with hexagon bases as seen in an image.

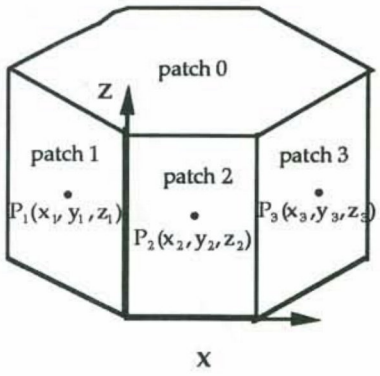

(a) The 3D coordinates of points to be reconstructed on each surface patch.

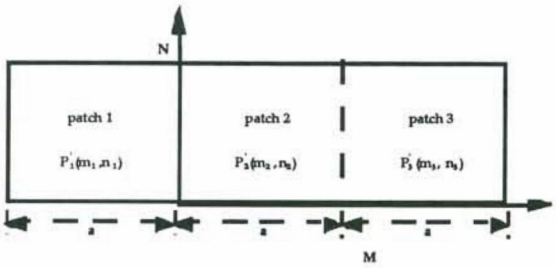

(b) The corresponding reconstructed 2D coordinates of points on the M-N plane.

Fig. 6 The reconstruction process for a regular prism with hexagon bases.

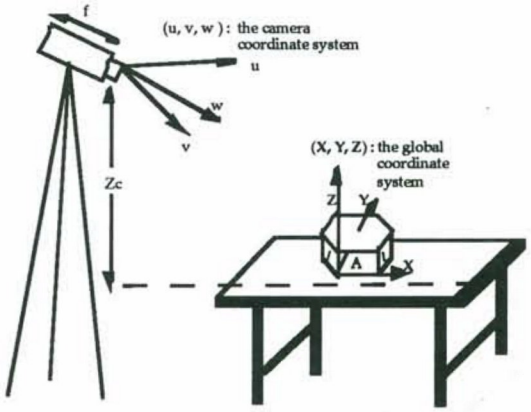

Fig. 7 The diagram of the experimental environments where f is the focus length and Z_c is the camera height (the difference between the height of the camera lens center and that of the table).

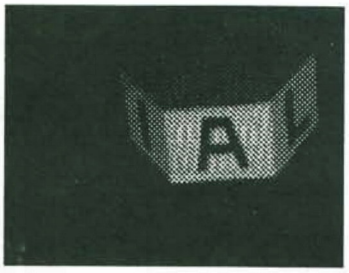

(a) Input image of regular prism 1.

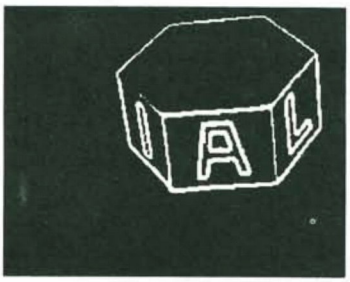

(b) Result of edge detection.

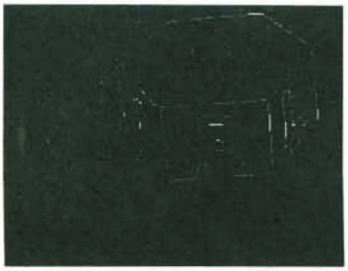

(c) Result of thinning.

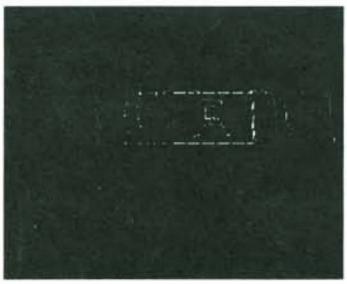

(d) Result of surface patch pattern reconstruction.

Fig. 8 Experimental results for regular prism 1 with character patterns on its surface patches.

Table 1. **Result of computed camera parameters and dimension parameters of the regular prisms (the actual values of a and b are 6.0, and 5.0, respectively; and the numbers in the parentheses are the error percents of the size).**

	object 1	object 2	object 3
f (pixel)	1011	1011	1011
X_c (cm)	7.38	12.72	11.62
Y_c (cm)	-52.90	-72.84	-62.63
Z_c (cm)	37.30	37.30	37.30
φ (°)	10.21	3.93	8.40
θ (°)	61.51	64.5	62.21
δ (°)	-6.82	-8.98	-7.74
a (cm)	5.84 (2.7 %)	6.16 (2.6 %)	5.91 (1.5 %)
b (cm)	5.21 (4.2 %)	4.82 (3.6 %)	5.11 (2.2 %)